Mar Biol (2016) 163:145
DOI 10.1007/s00227-016-2919-6

SHORT NOTES

Metabolomic analysis of competent larvae and juvenile veined rapa whelks (*Rapana venosa*)

Hao Song[1,2] · Li-Yuan Sun[3] · Zheng-Lin Yu[1,2] · Li-Na Sun[1] · Dong-Xiu Xue[1] · Tao Zhang[1] · Hai-Yan Wang[1]

Received: 21 March 2016 / Accepted: 20 May 2016 / Published online: 2 June 2016

Abstract Metamorphosis of a planktonic larval stage to a benthic juvenile is an important process in many marine invertebrates including the whelk, *Rapana venosa*, but understanding of the variety of molecular mechanisms underlying metamorphosis in different invertebrate clades is still poor. The present study examined the metabolic profiles of competent larval and post-larval stages of *R. venosa* using GC–MS. The whelk egg capsules were collected in Laizhou Bay, Shandong, China, in June 2015, and the larvae and post-larvae were cultured in the laboratory. A total of 263 metabolites were detected, 53 of which had different concentrations in larvae and post-larvae: 29 that were apparently higher following metamorphosis and 24 that were lower. Among the metabolites whose concentrations were higher in post-larvae, quinoline-4-carboxylic acid, the dipeptide cysteinylglycine, and anandamide were the most abundant. The metabolites present in higher concentrations in the competent larvae were a suite of oligosaccharides (maltotriose, glucose-6-phosphate, cellobiose, and maltose), L-homoserine, adrenosterone, and sarcosine. Although the roles of these and other metabolites in whelk development are not yet completely known, they provide some clues to the changes in energy metabolism and cell signaling that take place during metamorphosis.

Responsible Editor: J. Grassle.

Reviewed by Undisclosed experts.

Electronic supplementary material The online version of this article (doi:10.1007/s00227-016-2919-6) contains supplementary material, which is available to authorized users.

✉ Tao Zhang
tzhang@qdio.ac.cn

✉ Hai-Yan Wang
haiyanwang@qdio.ac.cn

[1] Institute of Oceanology, Chinese Academy of Sciences, 7 Nanhai Road, Qingdao 266071, Shandong, People's Republic of China

[2] University of Chinese Academy of Sciences, Beijing 100049, People's Republic of China

[3] Shandong Hydrobios Resources Conservation and Management Center, Yantai 264003, People's Republic of China

Introduction

The veined rapa whelk *Rapana venosa* has a typical biphasic life cycle similar to other mollusks. The crucial transition between the pelagic larval and benthic adult phases occurs in a relatively short time (~2–3 days) during the metamorphosis process (Pan et al. 2013) but involves complicated transformations of their digestive system, behavior, and physiology. The phytophagous larvae eventually reach the competent stage (30–33 days after hatching from the egg capsule), i.e., when the shell has four whorls and the velum is still present, the larvae occasionally sink to the bottom and explore the substrate with the developing foot. This signals that they are ready to settle and metamorphose into a carnivorous, benthic juvenile. Substantial morphologic changes occurring during metamorphosis include degeneration and resorption of the velum, proliferation and elongation of the foot, and rapid growth of the secondary shell (Pan et al. 2013). Moreover, molluscan metamorphosis is considered an important process in the context of evolution as animal metamorphosis is proposed to have arisen independently in different clade of animals (Hadfield 2000). Whelks are mostly marine gastropod mollusks in the clade Neogastropoda which includes more than 1500

species (Kantor 1996), and a comprehensive understanding of whelk metamorphosis is helpful in identifying the mechanisms of gastropod development and evolution. However, compared with the extensive studies on model organisms, such as zebrafish, *Drosophila* spp., and sea urchins (Heyland and Moroz 2006; Hodin 2006), current knowledge of the molecular mechanisms of gastropod metamorphosis is still limited and incomplete.

Discovery of chemical inducers that enable gastropods to initiate metamorphosis has gained much research attention. For the abalone *Haliotis rufescens*, competent larvae can be induced to metamorphose by γ-aminobutyric acid (GABA) and stereochemical compounds (Morse et al. 1979). Pharmacological evidence (Baloun and Morse 1984) suggests that GABAinergic neurons and GABA receptors play an important role in metamorphosis of *H. rufescens*, although the signal transduction pathway of the receptor is still unclear. Additional proteins and genes that are involved in gastropod settlement and metamorphosis have been investigated individually in recent years. Nitric oxide synthase (NOS) and Hsp90 were considered to participate in the metamorphosis of the mollusk *Haliotis asinina* owing to their pharmacological effect and mRNA expression pattern (Ueda 2013). NOS is detected as a positive metamorphic regulator in the larval foot of *H. asinina*, implicating chemo- and mechano-sensory roles in the initiation of metamorphosis (Ueda and Degnan 2014). More recently, transcriptome profiles of the early development of *R. venosa* revealed that some compounds, such as NOS, the 5-hydroxytryptamine receptor, IGF receptor, and EGF receptor, potentially participate in metamorphosis (Song et al. 2016).

The aforementioned studies reflect certain aspects of gastropod metamorphosis; however, understanding of the mechanisms underlying gastropod metamorphosis is still fragmentary. In addition, these studies have been more focused on mRNA or protein levels, and the study of metabolomics changes has been scarce, particularly for *R. venosa*. Considering the numerous, irreversible physical, physiological, and behavioral transformations (Leise et al. 2009), significant changes in metabolism must certainly occur. Metabolomics is the comprehensive analysis of metabolic profiles under a given set of conditions (Goodacre et al. 2004). Metabolomics has been used to investigate metamorphosis of North American bullfrogs *Rana catesbeiana*, where the approach proved useful (Ichu et al. 2014). To our knowledge, there has been no comprehensive metabolomics study of molluscan metamorphosis.

In the present study, we first performed comprehensive metabolomic analysis on competent larvae and post-larvae of the gastropod *R. venosa* using gas chromatography–mass spectrometry (GC–MS). We sought to reveal metabolites that may play roles in metamorphosis and provide comprehensive information on the underlying molecular mechanisms.

Materials and methods

Larval culture and sample preparation

Egg capsules of *Rapana venosa* were collected from Laizhou Bay (37°11′4.78″N, 119°41′3.75″E) in June 2015. Larval hatching and rearing were conducted at Blue Ocean Co. Limited (Laizhou, Shandong) according to Pan et al. (2013). Pelagic larvae were cultured in 3 m × 2 m × 1.5 m tanks with a density of 0.1 ind mL^{-1} with constant aeration and fed with *Platymonas subcordiformis*, *Isochrysis galbana*, and *Chlorella vulgaris* at 1.2×10^5 cells mL^{-1} $days^{-1}$. Seawater used for culturing was passed through a series of filters (sand and UV light) and exchanged twice daily. The water temperature was maintained at 24–26 °C and salinity at 29.8–31.7. Samples of the four-whorl larval stage (competent larvae) were collected on day 33 post-hatching. At this time, >95 % of the larvae were competent. On the same day, substrates with oyster juveniles (SL 400–600 μm, density 7 ind cm^{-2}) were put into the tanks to induce metamorphosis. Post-larvae were collected 3 days later following larval metamorphosis. We took ten replicate samples of competent larvae and post-larvae from the same batch, and each replicate sample was ~100 mg wet weight. The samples were immediately washed with dH_2O, snap frozen in liquid nitrogen, and stored at −80 °C until use.

GC–MS analysis

Sample pretreatment was performed according to an established method (Villas-Boâs et al. 2011). Briefly, ~60 mg of larvae or post-larvae from each sample were added with an internal standard (L-alanine-2,3,3,3-d4) to cold $MeOH/H_2O/CHCl_3$ (5:2:2; v/v/v). After homogenation and ultrasonic extraction, metabolites were derivatized with bis(trimethylsilyl)trifluoroacetamide (containing 1 % trimethylchlorosilane) and n-hexane to convert amino and non-amino organic acids into volatile carbamates and esters.

A 1-μL derivatized sample was injected into the GC–TOF/MS (Pegasus 4D LECO, USA) system for analysis. An Rtx-5MS capillary column (30 m × 250 μm I.D., J&W Scientific, Folsom, California) and FID detector were utilized. High-purity helium was used as the carrier gas at a flow rate of 1.0 mL min^{-1}. The temperature of the column was kept at 90 °C from 0 to 0.2 min, then slowly raised from 90 to 180 °C during 0.2–9.2 min, 180–240 °C from 21.2 to 23.2 min, 240– 280 °C from 23.2 to 34.2 min, and

then maintained at 280 °C during 23.2–34.2 min. The mass spectrometric conditions were as follows: EI ionization; electron energy, 70 eV. The temperature of the vaporizing chamber was 220 °C, and the injection port was 70 °C. Mass spectra were obtained from *m/z* 30–600, and the acceleration voltage was turned on after a solvent delay of 7.6 min.

Quality control samples and data analysis

We took 5 mg of larvae or post-larvae from each analytic sample and pooled them into a QC sample (100 mg). Three QC samples were constructed and were analyzed using the same method as the analytic samples. The QCs were injected at regular intervals (every ten samples) throughout the analytical run to provide a set of data from which repeatability was assessed.

The acquired raw GC–MS data were preprocessed by ChromaTOF software (v 4.34, LECO, St Joseph, Michigan). Briefly, after alignment with the Statistic Compare component, a CSV file with a three-dimensional data set, including sample information, retention time *m/z*, and peak intensities, was obtained. A total of 530 peaks (signal/noise >10) were detected in the samples. Then, we removed the internal standard and pseudo-positive peaks from the data set. After combining peaks that were ions of the same metabolite, a total of 263 metabolites were reliably identified. The data set matrix of these 263 metabolites was normalized using the sum intensity of the peaks in each sample. In this process, normalized values for some of the metabolites were 0 for certain stages. This was mainly because the metabolites were not present in certain stages or their concentration levels were undetectable. We therefore changed this value to one-tenth of the lowest concentration in the data (0.000001). Then, all the metabolite-normalized values were $\log_2$ transformed to calculate relative metabolite concentrations.

The SIMCA-P+ 14.0 software package (Umetrics, Umeå, Sweden) was used for analysis of the final data set. To investigate metabolic differences between competent larvae and post-larvae, *t* test statistics and fold-change values were calculated. In addition, principal component analysis (PCA) and (orthogonal) partial least squares discriminant analysis (O)PLS-DA were performed to visualize the metabolic differences between the experimental groups. PCA was carried out to reduce dimensionality and to assess the variation among the samples and between the groups. (O)PLS-DA helped to identify the metabolites that contributed the most toward sample partitioning between the two developmental stages. Variable importance in the projection (VIP) ranked the overall contribution of each variable to the (O)PLS-DA model, and the variables with VIP >1.0 are widely considered relevant for group discrimination. To assess the performance of the (O)PLS-DA model and guard against overfitting, the default 7-round cross-validation was applied with one-seventh of the samples being excluded from the mathematical model in each round.

Metabolite identification and screening metabolites with statistically significant abundance changes

Metabolites were annotated by linking ChromaTOF software to the available reference standards in our laboratory, the NIST 11 standard mass spectral database, and the Fiehn databases. A similarity score >70 % was used to consider metabolites as reference standards.

All of the significantly changed compounds in the post-larvae group were selected by comparing the compounds in the post-larvae group with the competent larva group using the abovementioned multivariate statistical analyses and the *t* test. Metabolites with both multivariate and univariate statistical significances (VIP >1.0 and $p < 0.05$) were selected as metabolites with significant changes. Also, the Kyoto Encyclopedia of Genes and Genomes (KEGG, http://www.genome.jp/kegg/) enrichment analysis of the metabolites with significant changes was implemented by MBRole (http://csbg.cnb.csic.es/mbrole/) (Chagoyen and Pazos 2011).

Results and discussion

Development and morphological characteristics of competent larvae and post-larvae

We observed the morphology and behavior of *R. venosa* larvae and post-larvae under the microscope. As shown in Fig. 1a, the major characteristics of the competent larvae are the ciliary velum and the primary shell with four spiral whorls (shell height (SH): 1.2–1.5 mm). The velum for swimming and ingestion degenerates and is reabsorbed during the metamorphic transition. Meanwhile, a secondary shell, more developed foot, and extensile eyestalks were the observable characteristics in the post-larvae (Fig. 1b). These morphological features were consistent with descriptions in Pan et al. (2013). As we observed, post-larvae of *R. venosa* had a SH of 1.5–2.5 mm and they prey only on juvenile bivalves. The transition from phytophagous to carnivorous feeding habits is an interesting phenomenon for further study.

General characteristics of GC–MS analysis

We overlapped the total ion chromatograms of the QC samples to assess the repeatability of the GC–MS analysis. The QC samples had reproducible retention times and mass

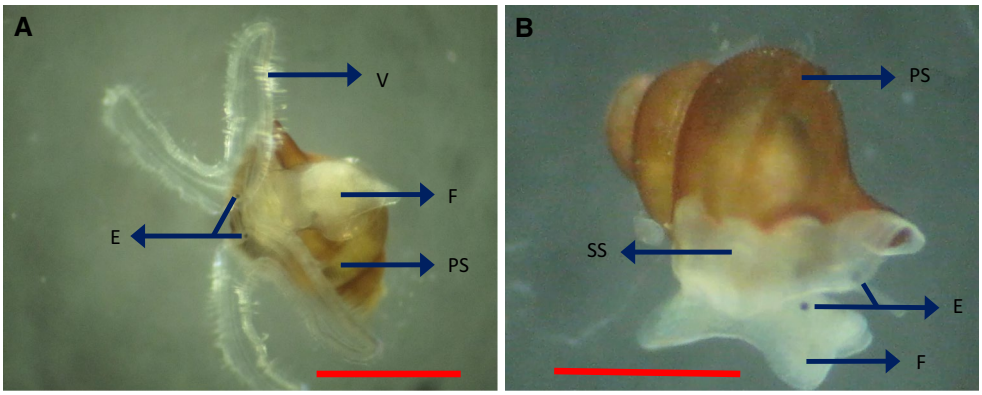

Fig. 1 Morphological characteristics of *R. venosa*. **a** Competent larva (30 days post-hatch, 25 °C) and **b** post-larva (3 days after metamorphosis induction, 25 °C). *E* eye, *F* foot, *PS* primary shell, *SS* secondary shell, *V* velum. *Red scale bar* 1 mm

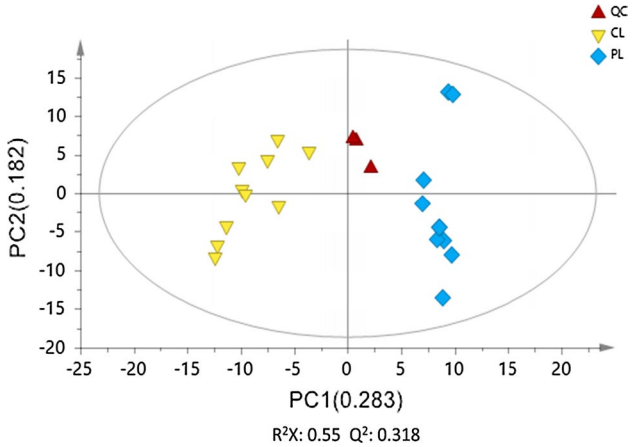

Fig. 2 Principal component analysis (PCA) score plot of metabolic profiles from competent larvae and post-larvae. PC1 (PC2) score represents the contribution of the first (second) principal component to explanatory ability of this PCA model. R^2X and Q^2 represent the explanatory ability and predictive ability of PCA, respectively. *Ellipse* represents 95 % confidence intervals. *QC* quality control samples, *CL* competent larvae, *PL* post-larvae. Both CL and PL have ten replicates

spectral peak intensities, which indicated that the pretreatment of samples and the GC–MS analysis method were stable and reliable. We detected 530 peaks in the samples from GC–MS analysis using ChromaTOF, from which the internal standards, pseudo-positive peaks, and redundancy were removed. The pseudo-positive peaks were mainly caused by noise, column bleeding, and/or BSTFA derivatization, whereas the redundancy was primarily caused by alkylation of certain metabolites with more than one active hydrogen that could participate in silylation reactions (DeHaven et al. 2010). After eliminating the unnecessary information, a total of 263 metabolites were reliably identified in the samples, and their relative concentrations were normalized and $\log_2$ transformed (Table S1).

As a first step in evaluating the final data sets, we performed PCA and compared samples from the two developmental stages. As a result (Fig. 2), the R^2X and Q^2 score in the PCA were 0.55 and 0.318, respectively. All of the sample plots include a 95 % confidence ellipse representing the Hotelling's T^2 test, and samples from the competent larval and post-larval stages were clearly different.

Metabolites in higher concentration after metamorphosis

There were 53 metabolites with significant differences in concentration between larvae and post-larvae: 29 that were higher in post-larvae (Table 1) and 24 that were higher in competent larvae (Table 2).

Among the metabolites, the concentration of quinoline-4-carboxylic acid in the post-larvae was the most significantly higher ($4.47E^{-10}$, Table 1). In recent studies, quinoline-4-carboxylic acid and its derivative are considered new immunosuppressive agents and are widely used in various medicinal applications, such as antifungal agents, antidrug resistant bacterial agents, antioxidant agents, anti-tubercular agents, and anticancer agents (Asahina and Takei 2012; Chatterjee et al. 2014; Bhatt et al. 2015). We suggest that quinoline-4-carboxylic acid plays an important role in the *R. venosa* immune system during the post-larval stage, as some studies have shown that the immune system is more mature and the immune response is stronger after metamorphosis of marine invertebrates, such as in the ascidian *Boltenia villosa* (Davidson and Swalla 2002) and mussel *Mytilus galloprovincialis* (Balseiro et al. 2013). The detected dipeptide cysteinylglycine, which is composed of cysteine and glycine, had a 45-fold increase after metamorphosis. It is derived from the incomplete breakdown of glutathione catabolism and considered an element in the extracellular antioxidant defense system (Ueland 1996).

Table 1 Metabolic profiles of *R. venosa* larvae whose abundance increased after metamorphosis

Metabolites	Mass	RT (min)	VIP value	*p* value	FC	Avg. (CL)	Avg. (PL)
Amino acid metabolism							
Cysteinylglycine	199	11.90	2.19	7.76E−06	45.61	0.015	0.667
Methionine sulfoxide	58	19.82	2.24	1.01E−04	41.27	0.313	12.925
2,6-Diaminopimelic acid	200	14.87	1.94	2.67E−04	14.20	0.0489	0.694
O-Acetylserine	188	26.21	2.06	5.74E−04	8.68	2.169	18.830
3-Hydroxypyruvate	166	10.59	1.55	3.99E−03	9.66	0.014	0.132
Synephrine	267	10.84	1.71	4.18E−03	6.82	0.038	0.256
Halostachine	116	12.19	1.40	7.73E−03	5.37E+05	0.000	0.537
5-Hydroxyindole-3-acetic acid	218	15.00	1.38	1.43E−02	21.74	0.011	0.238
N-carbamylglutamate	188	18.92	1.20	1.77E−02	8.84	0.134	1.180
Histidine	154	22.08	1.46	2.86E−02	7.33	6.209	45.511
Urea	189	12.07	1.24	3.25E−02	3.05	0.852	2.595
Dehydroascorbic acid	58	10.68	1.06	4.93E−02	3.15	2.536	7.992
Lipid metabolism							
15-Keto-prostaglandin f2alpha	103	25.86	1.86	1.75E−03	12.35	0.406	5.018
Phytosphingosine	204	15.26	1.81	2.78E−03	5.50	0.204	1.125
2,2-Dimethylsuccinic acid	57	30.94	1.65	6.01E−03	6.45	0.250	1.612
Androstanediol	91	34.42	1.41	7.84E−03	3.58E+05	0.000	0.358
Octadecanol	327	25.14	1.34	1.75E−02	6.89	0.050	0.343
Carbohydrate metabolism							
2-Deoxy-D-glucose	58	21.09	2.05	2.35E−04	3.17E+06	0.000	3.166
Fructose	103	21.57	1.65	3.70E−03	7.87	3.364	26.488
Nucleotide metabolism							
6-Hydroxynicotinic acid	180	25.06	2.13	3.79E−05	15.68	0.051	0.807
Uric acid	172	24.81	1.29	1.46E−02	10.67	0.187	1.999
Uridine	217	28.29	1.13	2.51E−02	6.91	1.287	8.894
Others							
Quinoline-4-carboxylic acid	84	10.94	1.02	4.47E−10	7.67	48.596	372.854
Glutaraldehyde	173	9.72	1.99	1.14E−05	1.05E+05	0.000	0.105
Anandamide	57	8.25	2.56	1.20E−05	1.28E+08	0.000	127.716
Formononetin	325	23.79	1.90	2.33E−04	6.25E+05	0.000	0.625
2-Butyne-1,4-diol	58	15.44	1.95	1.77E−03	2.17E+07	0.000	21.653
Vanillin	253	8.54	1.23	7.89E−03	4.14E+04	0.000	0.041
4-Vinylphenol dimer	61	11.09	1.06	2.37E−02	8.08	0.581	4.700

Mass, the mass value of fragment ions during quantitative measurement by mass spectrometry; RT, retention time; VIP value, variable importance in the projection; Avg. (CL) and Avg. (PL), average abundance of metabolites in competent larvae and post-larvae, respectively; FC, fold change of average abundance in PL versus CL

Anandamide was detected in very low concentration in the competent larvae, and it was significantly higher in the post-larvae (Table 1). As a type of potent, endogenous cannabinoid receptor agonist, anandamide has previously been detected in mollusks, such as the sea slug *Aplysia californica* (Di Marzo et al. 1999), the clam *Tapes decussatus*, the oyster *Crassostrea* sp., and the mussel *M. galloprovincialis* (Sepe et al. 1998). Moreover, anandamide and its receptor (CB1 receptor) were predominantly found in the ganglia of mollusks (Di Marzo et al. 1999). Interestingly, it has been reported that activation of the CB1 receptor is coupled to the production of nitric oxide (NO) in the mussel *Mytilus edulis* (Stefano et al. 1996), which can inhibit the release of presynaptic dopamine (Stefano et al. 1997). Studies have shown that NO and dopamine are pivotal in the regulation of many mollusk metamorphoses (Bonar et al. 1990; Leise et al. 2001; Ueda and Degnan 2013, 2014). In the ascidian *Herdmania momus*, NO has been demonstrated as a positive metamorphic regulator, but not in other ascidians (Ueda and Degnan 2013). Thus, further research on the impact of anandamide on the metamorphosis of *R. venosa* and other mollusks is of interest.

Table 2 Metabolic profiles of *R. venosa* larvae whose abundance decreased after metamorphosis

Metabolites	Mass	RT (min)	VIP value	*p* value	FC	Avg. (CL)	Avg. (PL)
Amino acid metabolism							
L-Homoserine	146	12.84	2.87	1.98E−31	7.70E+06	7.695	0.000
Sarcosine	116	10.52	1.38	3.06E−15	35.46	4565.764	128.767
3-Hydroxyanthranilic acid	220	12.41	2.00	3.71E−05	4.71	0.139	0.030
S-carboxymethylcysteine	58	16.23	1.32	2.02E−02	3.23	0.323	0.100
Oxoproline	156	22.90	1.30	2.80E−02	1.97	0.507	0.257
8-Aminocaprylic acid	67	28.82	1.24	4.91E−02	1.97	1.612	0.817
Lipid metabolism							
Cis-1,2-dihydronaphthalene-1,2-diol	191	8.51	2.59	7.99E−30	4.21E+05	0.421	0.000
Adrenosterone	90	10.91	2.65	6.56E−26	7.69E+05	0.769	0.000
2-Hydroxyvaleric acid	81	21.15	1.65	1.75E−03	2.79E+05	0.279	0.000
6-Phosphogluconic acid	299	28.36	1.66	1.75E−03	1.98E+05	0.198	0.000
D-Erythronolactone	217	22.84	1.60	5.81E−03	3.41	2.462	0.727
3,7,12-Trihydroxycoprostane	267	35.62	1.28	1.49E−02	2.70	0.204	0.076
Stigmasterol	97	33.61	1.48	2.14E−02	3.48	0.254	0.073
Carbohydrate metabolism							
Ribulose-5-phosphate	299	25.08	2.66	4.20E−24	9.37E+05	0.937	0.000
Maltotriose	204	31.75	2.76	3.93E−22	3.17E+06	3.168	0.000
Glucose-6-phosphate	299	27.69	2.00	8.61E−05	9.50	1.556	0.164
Cellobiose	204	32.24	1.76	1.81E−03	7.50	2.513	0.335
Maltose	231	32.00	1.06	3.10E−02	4.23	1.143	0.270
Others							
Tetracosane	73	25.54	2.43	4.86E−06	11.30	5.223	0.462
Trans-2-hydroxycinnamic acid	299	27.25	2.02	1.75E−05	15.37	0.112	0.007
Methylmalonic acid	180	10.41	1.71	3.61E−04	22.34	0.045	0.002
m-Cresol	165	10.72	1.55	1.75E−03	1.12E+05	0.112	0.000
Oxalic acid	175	16.22	1.57	6.26E−03	1.60	0.562	0.350
3-Indoleacetonitrile	215	10.69	1.52	7.70E−03	1.56E+05	0.156	0.000

Mass, the mass value of fragment ions during quantitative measurement by mass spectrometry; RT, retention time; VIP value, variable importance in the projection; Avg. (CL) and Avg. (PL), average abundance of metabolites in competent larvae and post-larvae, respectively; FC, fold change of average abundance in CL versus PL

Metabolites in lower concentration after metamorphosis

With the annotation information on these metabolites, we found that energy storage for metamorphosis in competent larvae is active. Among 24 metabolites whose concentrations were significantly higher in larvae (Table 2) were the oligosaccharides, including maltotriose, glucose-6-phosphate, cellobiose, and maltose. We speculate that this oligosaccharide enrichment occurred in the digestive tract and came from the micro-algal diet. During the process of molluscan metamorphosis, larvae experience tremendous morphological changes including loss of the velum, reorientation of the mouth and the foot, and growth of the shell and gill (Videla et al. 1998; Leise et al. 2009). These morphological changes require large amounts of energy, and larvae do not feed during metamorphosis. In the Chilean oyster, *Ostrea chilensis*, 64.5 % of the stored energy reserves in the competent larvae were consumed during metamorphosis (Videla et al. 1998). From another perspective, the abundance of oligosaccharides in the competent whelk larvae may simply reflect their gut contents.

The functions of some key metabolites in mollusk development are still unknown. L-homoserine and adrenosterone were detected at a high level in the competent larval stage but were absent after metamorphosis. Homoserine is a more reactive variant of the amino acid serine and is an intermediate in the biosynthesis of methionine, threonine, and isoleucine. Adrenosterone is a steroid hormone with a weak androgenic effect (Blasco et al. 2009). Moreover, the abundance of sarcosine dramatically dropped to only 3 % after metamorphosis. Sarcosine is a natural amino acid found in muscles and other body tissues and plays a role in the metabolism of choline to glycine.

KEGG enrichment of metabolites with statistically significant abundance changes

KEGG is a database resource for understanding high-level functions and utilities of biological systems, such as cells, organisms, and ecosystems, from molecular-level information. Therefore, we performed KEGG enrichment to identify metabolic pathways that were changed during *R. venosa* metamorphosis. As shown in Fig. 3, five pathways were significantly enriched ($p < 0.05$). The ABC transporter pathway was the most highly enriched ($p = 0.00268$), followed by the glycine, serine, and threonine metabolism pathway ($p = 0.00397$), the starch and sucrose metabolism pathway ($p = 0.00420$), the pyrimidine metabolism pathway ($p = 0.00670$), and the glyoxylate and dicarboxylate metabolism pathway ($p = 0.03420$). ABC transporters, also referred to as ATP-binding cassette transporters, make up one of the largest, widespread protein families found in both prokaryotic and eukaryotic organisms. These transporters couple with ATP hydrolysis to implement transport of various substrates (Higgins 2001). As shown in Fig. S1A, in the ABC transporter pathway, oligosaccharide, polyol, and lipid transporters pathway were significantly enriched as down-regulated, including maltose/maltodextrin, galactose oligomer/maltooligosaccharide, raffinose/stachyose/melibiose, glucoside, trehalose/maltose, and cellobiose transporters. The urea transporter pathway was significantly enriched as up-regulated. We speculate that the oligosaccharide enrichment occurred in the digestive tracts of the competent larvae feeding on micro-algae and believe this is worthy of further study and validation. More detailed information about the KEGG enrichment is available in Fig. S1.

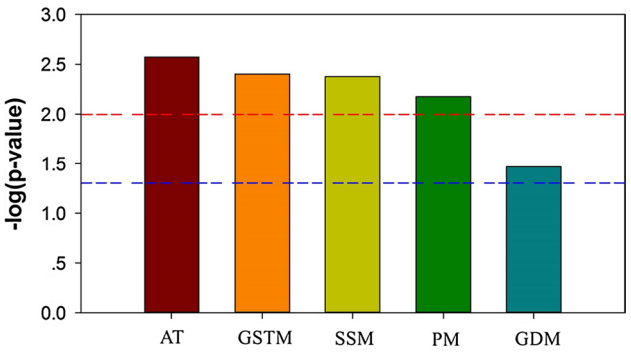

Fig. 3 KEGG pathway enrichment of metabolites with statistically significant abundance changes. *Horizontal axis* for the acronym of enriched pathway; *vertical axis* for the significance level of pathway enrichment. *AT* ABC transporters, *GSTM* glycine, serine, and threonine metabolism, *SSM* starch and sucrose metabolism, *PM* pyrimidine metabolism, *GDM* glyoxylate and dicarboxylate metabolism. Above the *red* and *blue dashed lines* represents $p < 0.01$ and $p < 0.05$, respectively

Using GC–MS in a carefully designed study with strict quality controls, we constructed comprehensive metabolomics profiles of *R. venosa* competent larvae and post-larvae. We identified important metabolites, such as anandamide and quinoline-4-carboxylic acid, that probably participate in mollusk metamorphosis according to the related cues in previous studies (Stefano et al. 1996, 1997; Di Marzo et al. 1999; Leise et al. 2001; Ueda and Degnan 2013). Their function in *R. venosa* metamorphosis still needs further research and verification. Our data provide significant clues to a better understanding of the regulation of development in *R. venosa* and identify key metabolites in important developmental processes. To our knowledge, this is the first metabolomics study on mollusk metamorphosis.

Acknowledgments The research was supported by the National Natural Science Foundation of China (Grant No. 31572636), the NSFC-Shandong Joint Fund for Marine Science Research Centers (Grant No. U1406403), the National Key Technology R&D Program of the Ministry of Science and Technology (Grant No. 2011BAD13B01), and the Agricultural Major Application Technology Innovation Project of Shandong Province. The funders had no role in the study design, data collection and analysis, decision to publish, or preparation of the manuscript.

Author contributions TZ and HW conceived and designed the experiments. HS and ZY performed the experiments. HS analyzed the data. TZ and HW contributed reagents, materials, and analysis tools. HS, LS, and DX wrote the paper.

Compliance with ethical standards

Conflict of interest Authors declare that he/she has no conflict of interest.

Human and animal rights All applicable international, national, and/or institutional guidelines for the care and use of animals were followed.

References

Asahina Y, Takei M (2012) 7-(4-substituted-3-cyclopropylaminomethyl-1-pyrrolidinyl) quinolonecarboxylic acid derivative. EP, US8106072

Baloun AJ, Morse DE (1984) Ionic control of settlement and metamorphosis in larval *Haliotis rufescens* (Gastropoda). Biol Bull 167:124–138

Balseiro P, Moreira R, Chamorro R, Figueras A, Novoa B (2013) Immune responses during the larval stages of *Mytilus galloprovincialis*: metamorphosis alters immunocompetence, body shape and behavior. Fish Shellfish Immunol 35:438–447

Bhatt HG, Agrawal YK, Patel MJ (2015) Amino-and fluoro-substituted quinoline-4-carboxylic acid derivatives: MWI synthesis, cytotoxic activity, apoptotic DNA fragmentation and molecular docking studies. Med Chem Res 24:1662–1671

Blasco M, Carriquiriborde P, Marino D, Ronco AE, Somoza GM (2009) A quantitative HPLC–MS method for the simultaneous determination of testosterone, 11-ketotestosterone and 11-β hydroxyandrostenedione in fish serum. J Chromatogr B 877:1509–1515

Bonar DB, Coon SL, Walch M, Weiner RM, Fitt W (1990) Control of oyster settlement and metamorphosis by endogenous and exogenous chemical cues. Bull Mar Sci 46:484–498

Chagoyen M, Pazos F (2011) MBRole: enrichment analysis of metabolomic data. Bioinformatics 27:730–731

Chatterjee A, Cutler SJ, Khan IA, Williamson JS (2014) Efficient synthesis of 4-oxo-4, 5-dihydrothieno [3, 2-c] quinoline-2-carboxylic acid derivatives from aniline. Mol Divers 18:51–59

Davidson B, Swalla BJ (2002) A molecular analysis of ascidian metamorphosis reveals activation of an innate immune response. Development 129:4739–4751

DeHaven CD, Evans AM, Dai H, Lawton KA (2010) Organization of GC/MS and LC/MS metabolomics data into chemical libraries. J Cheminform 2:194–204

Di Marzo V, De Petrocellis L, Bisogno T, Melck D (1999) Metabolism of anandamide and 2-arachidonoylglycerol: an historical overview and some recent developments. Lipids 34:S319–S325

Goodacre R, Vaidyanathan S, Dunn WB, Harrigan GG, Kell DB (2004) Metabolomics by numbers: acquiring and understanding global metabolite data. Trends Biotechnol 22:245–252

Hadfield MG (2000) Why and how marine-invertebrate larvae metamorphose so fast. Semin Cell Dev Biol 11:437–443

Heyland A, Moroz LL (2006) Signaling mechanisms underlying metamorphic transitions in animals. Integr Comp Biol 46:743–759

Higgins CF (2001) ABC transporters: physiology, structure and mechanism–an overview. Res Microbiol 152:205–210

Hodin J (2006) Expanding networks: signaling components in and a hypothesis for the evolution of metamorphosis. Integr Comp Biol 46:719–742

Ichu T-A, Han J, Borchers CH, Lesperance M, Helbing CC (2014) Metabolomic insights into system-wide coordination of vertebrate metamorphosis. BMC Dev Biol 14:335–348

Kantor YI (1996) Phylogeny and relationships of Neogastropoda. Origin and evolutionary radiation of the Mollusca. Oxford University Press, Oxford, pp 221–230

Leise EM, Thavaradhara K, Durham NR, Turner BE (2001) Serotonin and nitric oxide regulate metamorphosis in the marine snail *Ilyanassa obsoleta*. Am Zool 41:258–267

Leise EM, Froggett SJ, Nearhoof JE, Cahoon LB (2009) Diatom cultures exhibit differential effects on larval metamorphosis in the marine gastropod *Ilyanassa obsoleta* (Say). J Exp Mar Biol Ecol 379:51–59

Morse DE, Hooker N, Duncan H, Jensen L (1979) γ-Aminobutyric acid, a neurotransmitter, induces planktonic abalone larvae to settle and begin metamorphosis. Science 204:407–410

Pan Y, Qiu T, Zhang T, Wang P, Ban S (2013) Morphological studies on the early development of *Rapana venosa*. J Fish China 37:1503–1512 **(in Chinese)**

Sepe N, De Petrocellis L, Montanaro F, Cimino G, Di Marzo V (1998) Bioactive long chain N-acylethanolamines in five species of edible bivalve molluscs: possible implications for mollusc physiology and sea food industry. Biochim Biophys Acta 1389:101–111

Song H, Yu ZL, Sun LN, Gao Y, Zhang T, Wang HY (2016) De novo transcriptome sequencing and analysis of *Rapana venosa* from six different developmental stages using Hi-seq 2500. Comp Biochem Phys D 17:48–57

Stefano GB, Liu Y, Goligorsky MS (1996) Cannabinoid receptors are coupled to nitric oxide release in invertebrate immunocytes, microglia, and human monocytes. J Biol Chem 271:19238–19242

Stefano GB, Salzet B, Rialas CM, Pope M, Kustka A, Neenan K, Pryor S, Salzet M (1997) Morphine-and anandamide-stimulated nitric oxide production inhibits presynaptic dopamine release. Brain Res 763:63–68

Ueda N (2013) A transcriptional perspective of NOS and HSP90 gene activity during phylogenetically divergent marine invertebrate metamorphosis. Ph.D. Thesis, University of Queensland

Ueda N, Degnan SM (2013) Nitric oxide acts as a positive regulator to induce metamorphosis of the ascidian *Herdmania momus*. PLoS One 8:e72797.1–e72797.16

Ueda N, Degnan SM (2014) Nitric oxide is not a negative regulator of metamorphic induction in the abalone *Haliotis asinina*. Front Mar Sci 1, Article 21:1–13

Ueland PM (1996) Reduced, oxidized and protein-bound forms of homocysteine and other aminothiols in plasma comprise the redox thiol status. J Nutr 126:1281S–1284S

Videla J, Chaparro O, Thompson R, Concha I (1998) Role of biochemical energy reserves in the metamorphosis and early juvenile development of the oyster *Ostrea chilensis*. Mar Biol 132:635–640

Villas-Bôas SG, Smart KF, Sivakumaran S, Lane GA (2011) Alkylation or silylation for analysis of amino and non-amino organic acids by GC-MS? Metabolites 1:3–20